atmosphere

MDPI

Article

Seasonal Characteristics of Atmospheric $PM_{2.5}$ in an Urban Area of Vietnam and the Influence of Regional Fire Activities

Quang Trung Bui [1,2], Duc Luong Nguyen [1,2,*] and Thi Hieu Bui [1,2]

[1] Faculty of Environmental Engineering, Hanoi University of Civil Engineering (HUCE), 55 Giai Phong, Hanoi 100000, Vietnam
[2] Research Group for Clean Air Solutions (ReCAS), Hanoi University of Civil Engineering (HUCE), 55 Giai Phong, Hanoi 100000, Vietnam
* Correspondence: luongnd@huce.edu.vn

Abstract: This study investigated the seasonal variation and chemical characteristics of atmospheric $PM_{2.5}$ at an urban site in Hanoi City of Vietnam in summer (July 2020) and winter (January 2021) periods. The study results showed that the average value of daily $PM_{2.5}$ concentrations observed for the winter period was about 3 times higher than the counterpart for the summer period. The concentrations of major species in atmospheric $PM_{2.5}$ (SO_4^{2-}, NH_4^+, K^+, OC and EC) measured during the winter period were also significantly higher than those during the summer period. The contribution of secondary sources to the measured OC (the largest contributor to $PM_{2.5}$) was larger than that of primary sources during the winter period, compared to those in the summer period. The correlation analysis among anions and cations in $PM_{2.5}$ suggested that different sources and atmospheric processes could influence the seasonal variations of $PM_{2.5}$ species. The unfavorable meteorological conditions (lower wind speed and lower boundary layer height) in the winter period were identified as one of the key factors contributing to the high $PM_{2.5}$ pollution in this period. With the predominance of north and northeast winds during the winter period, the long-range transport of air pollutants which emitted from the highly industrialized areas and the intensive fire regions in the southern part of China and Southeast Asia region were likely other important sources for the highly elevated concentrations of $PM_{2.5}$ and its chemical species in the study area.

Keywords: atmospheric $PM_{2.5}$; chemical compositions; sources and processes; seasonal meteorological condition; regional fires; long-range transport; Hanoi

Citation: Bui, Q.T.; Nguyen, D.L.; Bui, T.H. Seasonal Characteristics of Atmospheric $PM_{2.5}$ in an Urban Area of Vietnam and the Influence of Regional Fire Activities. *Atmosphere* **2022**, *13*, 1911. https://doi.org/10.3390/atmos13111911

Academic Editors: Hiroshi Hayasaka and Antonio Donateo

Received: 21 September 2022
Accepted: 13 November 2022
Published: 16 November 2022

1. Introduction

Long-term and short-term exposure to $PM_{2.5}$ (fine particles with aerodynamic diameter < 2.5 μm) could cause adverse health impacts, as pointed out by previous studies [1,2]. The possible sources and transformation process of aerosols in the atmosphere could be identified by analyzing the chemical compositions of $PM_{2.5}$ [3]. Anthropogenic species, such as sulphate (SO_4^{2-}), nitrate (NO_3^-), and ammonium (NH_4^+), have been generally reported as the main components of atmospheric aerosols [4]. SO_4^{2-} and NO_3^- can be formed through the oxidation of SO_2 and NOx, respectively, which are released from anthropogenic sources (e.g., industry, power plants, traffic emissions). According to [4], NO_3^- exists in both aerosol and gaseous phases (in the form of nitric acid vapor), while SO_4^{2-} is only found in the aerosol phase. NH_3 which is emitted from various sources (i.e., livestock and fertilizer, industrial activities, traffic emission) can react with acidic aerosols to form the neutralized ammonium salts (e.g., NH_4NO_3, $(NH_4)_2SO_4$, NH_4HSO_4) in the atmosphere [5,6]. The other species in $PM_{2.5}$ including carbonaceous components (organic carbon (OC) and elemental carbon (EC)) and potassium (K^+) have been commonly considered as the tracers of biomass burning [7]. Since $PM_{2.5}$ secondary species have been realized to have negative effects on both human health and the climate [8], the understanding of

$PM_{2.5}$ chemical compositions in particular areas plays an important role in formulating air quality management policies and strategies.

According to [9], in the big cities of Vietnam, such as Ho Chi Minh City and Hanoi, heavy air pollution usually occurs, which can pose severe health risks. Hanoi is the second largest city and the capital of Vietnam, with a population of about 8.25 million people. During recent years, the rapid urban population growth, urbanization, economic development, and motorization might have contributed significantly to the increased air pollution in Hanoi [10]. There was an increasing trend of $PM_{2.5}$ pollution in Hanoi during the period of 2017–2020 [11]. Recently, heavily polluted events with significantly high $PM_{2.5}$ concentrations occurred more frequently in Hanoi, especially during the transition and winter seasons when the unfavorable meteorological conditions were endured [12]. Key sources of air pollution in Hanoi were reported, including transportation, industry, domestic coal combustion, open burning of biomass, and long-range transported air pollutants [11]. It was reported that traffic emission was one of the largest contributors to urban air pollution in Hanoi [13]. The number of private vehicles (mainly cars and motorcycles) has been increasing from year to year in Hanoi. According to [14], there were 787,000 cars and about 6 million motorcycles in Hanoi by the end of 2019. The strong impact of traffic emission on local air pollution in Hanoi was also indicated by the trend of increased concentrations of NOx and CO during rush hours in the morning and evening [15]. In addition to the primary emission sources as mentioned above, secondary aerosol has been pointed out as one of the significant sources of $PM_{2.5}$ pollution in Hanoi as well [10]. On the other hand, the local $PM_{2.5}$ pollution in Hanoi could be also impacted by other factors (i.e., pattern of air mass, local/regional fire sources) that could vary from season to season. Although fire activities have been reported as one of the major sources of air pollution in Southeast Asia [10], the seasonal impact of fire sources on the $PM_{2.5}$ pollution in Hanoi is poorly understood. Moreover, due to the impact of climate change, the frequency of fire activities might be increased, which could exacerbate the local air pollution. In the situation of increased $PM_{2.5}$ pollution in Hanoi, it is of significance to investigate the seasonal variation and chemical characteristics of atmospheric $PM_{2.5}$ to gain a better understanding of how the key sources and atmospheric processes affecting $PM_{2.5}$ are measured in Hanoi. Recently, the government of Vietnam has approved the National Plan on Air Quality Management for the Period of 2021–2025, in which one of the key solutions was the implementation of scientific research to identify the contribution of different emission sources to $PM_{2.5}$ pollution and to provide strong evidence for the government to develop robust air quality management policies and strategies towards reducing $PM_{2.5}$ pollution and protecting public health. In response to this demand, this study aimed to (1) investigate the seasonal variation of mass concentration and chemical characteristics of $PM_{2.5}$ measured in an urban area of Hanoi City; (2) analyze the relationship among $PM_{2.5}$ chemical compositions and identify the key sources and atmospheric processes impacting the seasonal variation of atmospheric $PM_{2.5}$ and its components; and (3) investigate the influences of seasonal meteorological conditions and regional fire activities on the characteristics of $PM_{2.5}$ and its components.

2. Materials and Methods

2.1. Sampling Site

In the present study, the $PM_{2.5}$ sampling site was situated on the roof of the two-floor building of the Hanoi University of Civil Engineering, 55 Giai Phong Road, Hai Ba Trung District in Hanoi (Figure 1). The sampling site (Lat 21.003 N, Long 105.842 E) was considered as an urban mixed site that was impacted by various anthropogenic sources such as motor vehicle emission, construction activities, and nearby industrial activities. There are many significant anthropogenic emission sources in the areas surrounding Hanoi, such as the steel, cement, and coal-fired power plants which are situated in the east, southeast, and north directions (Figure 1). When wind is blowing from these directions, air pollutants originating from those sources could be transported to the study area in Hanoi [10].

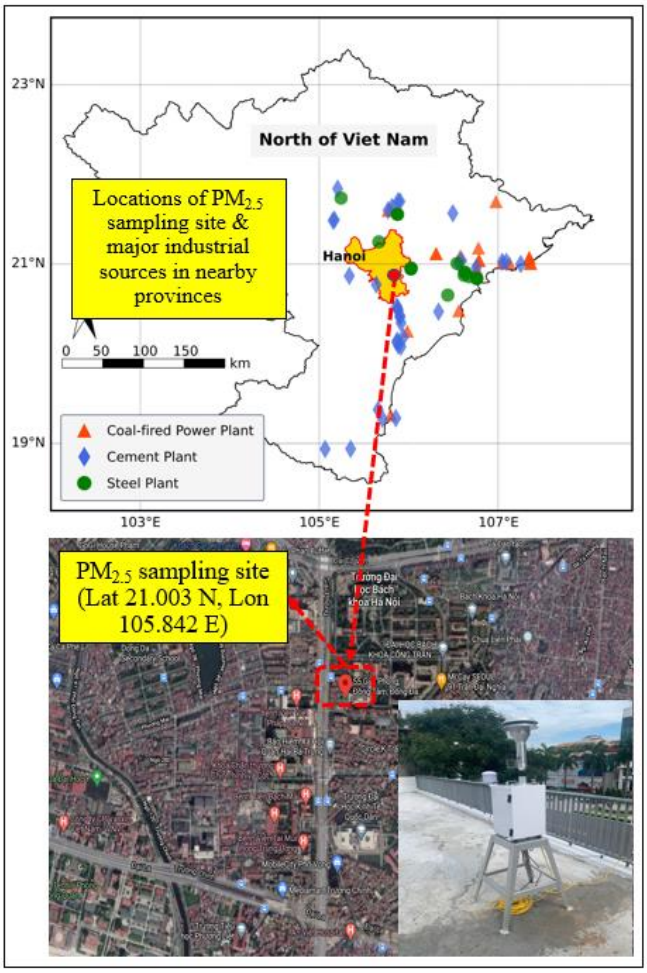

Figure 1. Study area and sampling site for $PM_{2.5}$ measurement in Hanoi, Vietnam.

2.2. $PM_{2.5}$ Sampling and Chemical Analysis

The two intensive 24-h integrated $PM_{2.5}$ sampling campaigns were carried out daily during the summer (from 8 to 30 July 2020) and winter (from 5 to 30 January 2021) periods. A total of eighteen (for summer) and seventeen (for winter) 24-h $PM_{2.5}$ samples were obtained using Whatman quartz fiber filters which were placed in an air sampler (Met One E-FRM-200, Grants Pass, OR, USA) operated at a flow rate of 16.7 L/min. Before sampling, the filters were heated at 900 °C in an electric furnace for three hours to remove carbonaceous contaminants. After sampling, the filters were brought to the laboratory and stored in the refrigerator at 4 °C to avoid the evaporation of volatile constituents before performing chemical analysis. Field blanks were also collected using the procedures, identical to those applied for collecting $PM_{2.5}$ samples, however without operating the air sampler. Before and after sampling, the filters were weighed gravimetrically to determine the $PM_{2.5}$ total mass. The filters were equilibrated for 48 h in a climate-controlled room prior to pre- and post-weighing. During the equilibration period, the relative humidity and air temperature in the weighing room were maintained at about 40% and 22 °C, respectively. Prior to weighing, the balance weighing chamber was cleaned by a fine brush. The surfaces near the micro-balance were also cleaned with alcohol-moistened disposable laboratory wipes. The filters were placed on the balance pan for at least 30 s and the mass data was then recorded. Each filter was weighed three times.

Water-soluble inorganic ions (WSIIs) consisting of Na^+, NH_4^+, K^+, Mg^{2+}, Ca^{2+}, Cl^-, F^-, SO_4^{2-}, NO_3^-) in $PM_{2.5}$ were determined using ion chromatography (IC, Thermo Scientific, Waltham, MA, USA, Dionex 600). A piece of filter sample was placed in the

Erlenmeyer flask with 10 mL of ultra-pure water and treated in the ultrasonic cleaner for about 30 min. The extract was then filtrated through 0.45 μm nylon syringe filters and injected to the IC. The AS4A-SC analytical column (4 × 250 mm) was employed to analyze anions with the eluent of 1.8 mM Na_2CO_3 and 1.7 mM $NaHCO_3$ (flow rate of 2 mL/min). The CS12A analytical column (2 × 250 mm) was utilized to analyze cations with the eluent mixture of 22 mM H_2SO_4 (flow rate of 0.25 mL/min). The Dionex IC injection volume (25 μL), column temperature (35 °C), and run time (30 min) were kept the same for the chemical analysis of both cations and anions. The blank filters were routinely analyzed to remove contaminants from blank filters using the same procedures applied for the field samples, and the results were subtracted from the sample values.

The analysis of carbonaceous species (OC and EC) in $PM_{2.5}$ was performed following the NIOSH 870 thermal/optical transmittance protocol using the carbon analyzer (Model 5L, Sunset Laboratory Inc., Portland, OR, USA). A piece of filter sample was heated in the quartz oven at different temperatures (310, 475, 615, and 870 °C) in the pure helium (oxygen-free environment) to analyze four OC fractions (OC1, OC2, OC3, and OC4). The temperature of the oven was then decreased to 550 °C and six fractions of EC including EC1, EC2, EC3, EC4, EC5, and EC6 were determined by subsequently heating at 550, 625, 700, 775, 850, and 870 °C in the environment of 98% He and 2% O_2. The carbon vapour from the heating process was oxidized to carbon dioxide (CO_2) in the oxidation oven. The CO_2 was then reduced to methane (CH_4) in nickel catalyst and quantitatively measured with a flame ionization detector. The instrument's detection limit was 0.1 μg C/cm^2 and the analytical uncertainty was equal to ±(OC/EC concentration × 0.05) + instrument blank concentration.

2.3. Meteorological Data

The ERA5 reanalysis data for hourly meteorological parameters (wind direction, wind speed, relative humidity, ambient temperature, and boundary layer height) obtained from the European Centre for Medium-Range Weather Forecasts (https://cds.climate.copernicus.eu, accessed on 15 March 2021) was extracted for the study area in Hanoi and used to assess the influence of seasonal meteorological condition on the variation of $PM_{2.5}$ and its components.

2.4. MODIS Fire Radiative Power Data

In order to identify biomass burning regions in the Asia region and assess their effect on the variation of $PM_{2.5}$ and its components measured in the study area, the cumulative fire radiative power (FRP) data acquired from NASA's FIRMS website (https://www.earthdata.nasa.gov/learn/find-data/near-real-time/firms, accessed on 15 March 2021) was used. The FRP data was derived by the MODIS Collection 6 active fire-detection algorithm [16].

2.5. Air Mass Backward Trajectories

In the present study, the analysis of three-day air mass backward trajectories arrived at the sampling site in Hanoi was carried out to identify and assess the likely impact of fire source regions in the Asia region to $PM_{2.5}$ and its components measured in Hanoi. Three days were expected to be enough time for most trajectories to pass through possible source regions in the Asia region. The web-based version of the hybrid single-particle Lagrangian integrated trajectory (HYSPLIT) model [17] provided at https://www.ready.noaa.gov/HYSPLIT.php (accessed on 15 March 2021) and NCEP GDAS data was employed to generate the air mass backward trajectories. The starting height of 1500 m above-ground level was selected and air mass trajectories were calculated every 1 h.

3. Results and Discussion

3.1. Seasonal Variation of Concentrations of $PM_{2.5}$ and Its Chemical Compositions

The daily mean $PM_{2.5}$ concentrations and meteorological parameters observed in the study area during the summer and winter periods are expressed in Figure 2. For the summer period, there were five measurement days (out of eighteen measurement days) where the daily concentrations of $PM_{2.5}$ were higher than the corresponding value for $PM_{2.5}$ (50 μg m^{-3}) regulated by the national standard for ambient air quality. For the winter period, the daily concentrations of $PM_{2.5}$ were much higher than the national standard for all measurement days, which clearly indicated heavy $PM_{2.5}$ pollution. Especially for several days in the winter period, the daily concentrations of $PM_{2.5}$ were over 200 μg m^{-3}. The statistical values of $PM_{2.5}$ total mass, $PM_{2.5}$ chemical compositions, and meteorological conditions during the summer and winter measurement periods were summarized in Table 1. The average value (40.20 μg m^{-3}) for the daily $PM_{2.5}$ concentrations estimated for the summer period was about 3 times lower than the counterpart (122.90 μg m^{-3}) for the winter period. Compared to those reported for the urban areas in the other Asian countries (Table 2), the average value of $PM_{2.5}$ concentration (80.37 ± 55.63 μg m^{-3}) estimated for the whole study period in Hanoi was much higher than those for Kampar [18], Kuala Lumpur [19], and Johor Bahru [20,21] in Malaysia; Singapore [22]; Bangkok, Thailand [23]; Bandung, Indonesia [24]; Ho Chi Minh City, Vietnam [25]; Shanghai, China [26]; and Beijing, China [27]. Even compared to those measured during the smoke haze periods in Kuala Lumpur, Malaysia [19] and Chiang Mai, Thailand [28], the average value of $PM_{2.5}$ concentration observed in Hanoi in this study was still relatively higher. However, compared to those observed for several urban areas in India, the $PM_{2.5}$ concentration measured in Hanoi was lower than the values reported for Chandigarh [29], Delhi, Varanasi, and Kolkata [30].

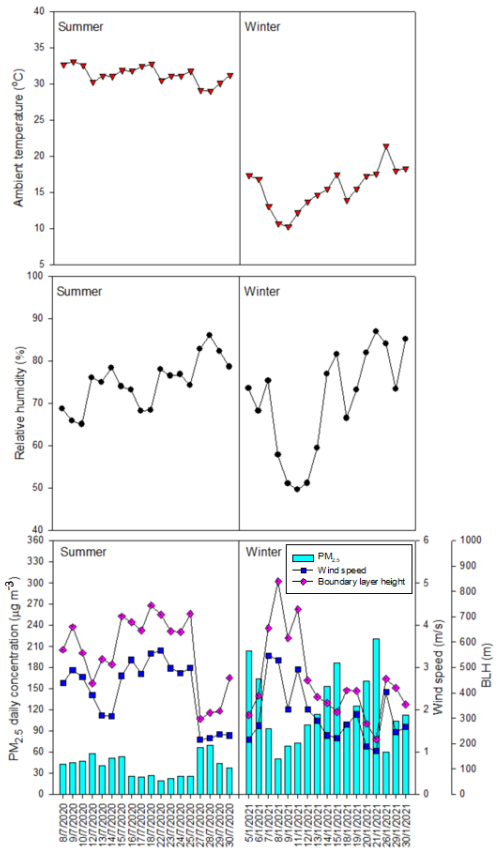

Figure 2. $PM_{2.5}$ daily mean concentration and meteorological conditions for the summer and winter periods.

Table 1. Statistical summary of daily $PM_{2.5}$ measurement and meteorological conditions.

	Mean ± Standard Deviation (Range)		
	Summer	**Winter**	**All Data**
$PM_{2.5}$ and its chemical compositions (μg m^{-3})			
$PM_{2.5}$	40.20 ± 15.36 (19.79–69.92)	122.90 ± 50.88 (49.83–220.41)	80.37 ± 55.63 (19.79–220.41)
F^-	0.12 ± 0.02 (0.05–0.14)	0.02 ± 0.009 (0.008–0.039)	0.07 ± 0.05 (0.008–0.14)
Cl^-	0.21 ± 0.20 (0.03–2.06)	2.19 ± 1.04 (0.54–4.49)	1.17 ± 1.28 (0.03–4.49)
NO_3^-	0.85 ± 1.24 (0.14–4.86)	0.018 ± 0.009 (0.005–0.043)	0.44 ± 0.47 (0.01–4.86)
SO_4^{2-}	3.63 ± 2.60 (0.87–10.44)	10.28 ± 7.41 (1.71–27.17)	6.86 ± 6.37 (0.87–27.17)
Na^+	0.31 ± 0.07 (0.20–0.45)	0.21 ± 0.09 (0.08–0.39)	0.26 ± 0.09 (0.08–0.45)
NH_4^+	1.45 ± 1.32 (0.32–4.98)	4.05 ± 2.60 (0.74–10.42)	2.71 ± 2.40 (0.32–10.42)
K^+	0.41 ± 0.25 (0.10–1.12)	1.04 ± 0.52 (0.37–1.90)	0.72 ± 0.51 (0.10–1.90)
Mg^{2+}	0.09 ± 0.10 (0.03–0.47)	0.06 ± 0.03 (0.01–0.11)	0.07 ± 0.07 (0.01–0.47)
Ca^{2+}	0.47 ± 0.25 (0.19–0.98)	0.47 ± 0.20 (0.17–0.88)	0.47 ± 0.22 (0.17–0.98)
EC	1.34 ± 0.77 (0.27–2.79)	2.40 ± 0.90 (1.07–3.96)	1.85 ± 0.98 (0.27–3.96)
OC	11.85 ± 6.43 (4.74–28.20)	30.20 ± 12.01 (12.80–52.07)	20.76 ± 13.23 (4.74–52.07)
Trace elements (*)	1.98 ± 0.78 (0.82–3.69)	1.25 ± 0.49 (0.29–2.20)	1.62 ± 0.74 (0.29–3.69)
Meteorology			
Wind speed (m/s)	2.46 ± 0.73 (1.29–3.41)	1.88 ± 0.69 (1.02–3.28)	2.18 ± 0.76 (1.02–3.41)
Boundary layer height (m)	563.93 ± 143.71 (296.77–745.62)	447.12 ± 167.48 (215.94–840.02)	507.19 ± 164.42 (215.94–840.02)
Ambient temperature (°C)	31.32 ± 1.19 (29.01–33.09)	15.51 ± 2.95 (10.24–21.39)	23.64 ± 8.31 (10.24–33.09)
Relative humidity (%)	74.91 ± 5.91 (65.06–86.01)	70.36 ± 12.51 (49.63–86.96)	72.70 ± 9.82 (49.63–86.96)

Note: (*) Trace elements including Al, Ti, V, Cr, Mn, Fe, Co, Ni, Cu, Zn, Sr, Mo, Ag, Cd, Sb, Ba, Pb.

Table 2. Comparison of $PM_{2.5}$ concentrations in this study and other studies.

Location, Country	**Type of Sampling Site**	**Study Period**	**$PM_{2.5}$ Concentration (μg m^{-3})**	**References**
Kampar, Malaysia	Semi-Urban	August–October 2015	55.89	[18]
Kuala Lumpur, Malaysia	Urban	June 2015–January 2016		[19]
		-Pre-haze period	24.5 ± 12.0	
		-Haze period	72.3 ± 38.0	
		-Post-haze period	14.3 ± 3.58	
Johor Bahru, Malaysia	Suburban	August 2017–January 2018 (Southwest monsoon)	21.85	[20]
Johor Bahru, Malaysia	Urban	January–March 2019	26.28 ± 4.32	[21]
Singapore	Urban	November 2015–February 2016	13.02 ± 2.73	[22]
Bangkok, Thailand	Urban	August 2017–March 2018	77.0 ± 21.2	[23]
Bandung, Indonesia	Urban	May 2012–December 2017	18 ± 8	[24]
Ho Chi Minh, Vietnam	Urban roadside	March 2017–March 2018	36.3 ± 13.7	[25]
Shanghai, China	Urban	May 2018–March 2019	39.35 ± 35.74	[26]
Beijing, China	Urban	December 2018–November 2019	66.58 ± 60.17	[27]
Chiang Mai, Thailand	Urban	March–April 2016 (Smoke haze period)	65.3 ± 17.6	[28]
Chandigarh, India	Urban	October–November 2015 (Haze period)	161.7	[29]
Delhi, India	Urban		135 ± 64	
Varanasi, India	Urban	January 2015–December 2016	99 ± 33	[30]
Kolkata, India	Urban		116 ± 38	
Hanoi, Vietnam	Urban	July 2020 and January 2021	80.37	This study

With respect to the seasonal meteorological conditions (Table 1), the average values for daily wind speed, boundary layer height, ambient temperature, and relative humidity estimated for the summer period were about 1.31, 1.26, 2.02, and 1.06 times higher than the counterparts for the winter period. It was seen that the values of wind speed, relative humidity, boundary layer height, and ambient temperatures varied from day to day in

both the summer and winter measurement periods (Figure 2). The daily variation trend of boundary layer height and wind speed was somewhat similar in both the summer and winter period. Further discussion on the impact of seasonal meteorological conditions on the variation of $PM_{2.5}$ and its components are provided in a later section of this paper.

Figure 3 shows the daily mean concentrations for $PM_{2.5}$ chemical species. As displayed in Figure 3 and Table 1, WSII (Cl^-, NO_3^-, SO_4^{2-}, Na^+, NH_4^+, K^+, and Ca^{2+}) and carbonaceous species (OC and EC) were recognized as the major components in $PM_{2.5}$ in the study area. The total mass concentrations of WSII and carbonaceous species accounted for about 52.71 ± 20.82% (range 20.26–82.39%) and 41.28 ± 7.27% (range 24.37–56.14%) of the total $PM_{2.5}$ mass concentrations for the summer and winter periods, respectively. For the summer period, the mean concentrations of the four major anions followed the sequence of $SO_4^{2-} > NO_3^- > Cl^- > F^-$, while the five major cations ranked in the order of $NH_4^+ > Ca^{2+} > K^+ > Na^+ > Mg^{2+}$. However, for the winter period, those orders were $SO_4^{2-} > Cl^- > F^- > NO_3^-$ and $NH_4^+ > K^+ > Ca^{2+} > Na^+ > Mg^{2+}$. Among the WSII species, SO_4^{2-} and NH_4^+ were the most dominant ones in both seasons, in which their concentrations accounted for 67.5% and 78.2% of total concentrations of WSII species in the summer and winter periods, respectively. The average values for daily concentration of Cl^-, SO_4^{2-}, NH_4^+, and K^+ measured during the winter period were significantly higher than those during the summer period. On the other hand, a contrasting seasonal pattern was seen for F^-, NO_3^-, Na^+, and Mg^{2+} (Table 1).

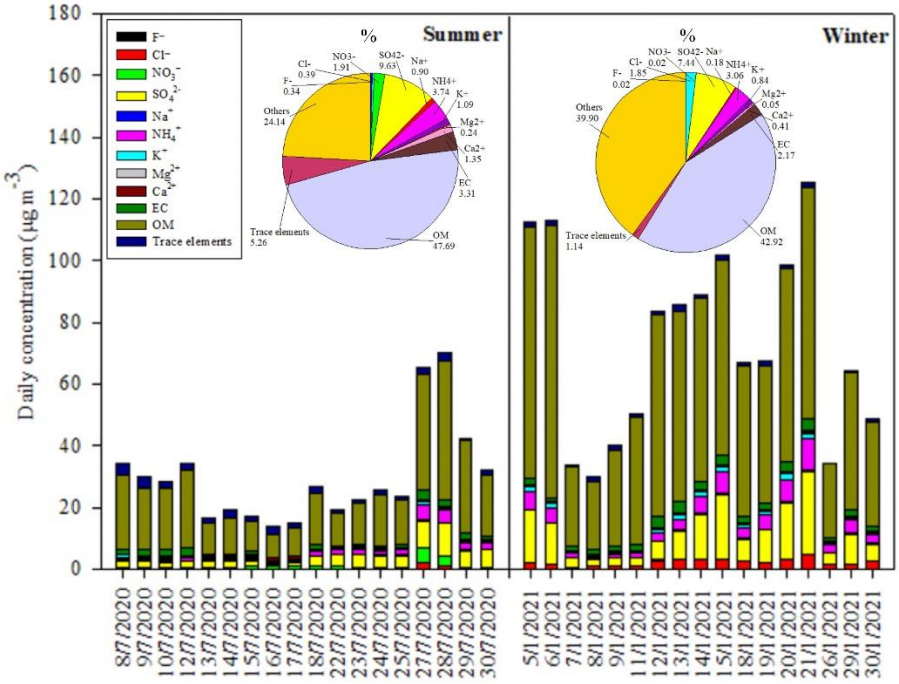

Figure 3. Daily $PM_{2.5}$ chemical composition measured at the sampling site for the summer and winter periods.

OC was clearly seen to be the largest contributor to total mass of $PM_{2.5}$, which were 29.81 ± 9.70% and 25.25 ± 5.99% for the summer and winter periods, respectively. The mean value ± standard deviation for daily concentrations of OC for the winter period was 30.20 ± 12.01 μg m^{-3} (range 12.80–52.07 μg m^{-3}), which was much higher than the counterpart for the summer period (mean value ± standard deviation of 11.85 ± 6.43 μg m^{-3}, range 4.74–28.20 μg m^{-3}). These results indicated the elevated concentration and large variability of OC during the winter period, owing to its complex sources (both primary and secondary ones) as investigated in the later sections. The mean value for daily concentrations of EC in the winter period was also 1.8 times higher than that in the summer period. The elevated concentrations of carbonaceous species, especially OC, contributed

largely to the high pollution of $PM_{2.5}$ during the winter period. Since OC was the largest contributor to $PM_{2.5}$ for both seasons, this study further investigated the contribution of primary organic carbon (POC) and secondary organic carbon (SOC) to the measured OC. It is well known that OC could be directly released as POC from various sources such as natural and geological activities, industrial emissions, and fuel combustions. OC could be also found in the form of SOC when the chemical transformation of semi-volatile as well as volatile organic compounds and the nucleation or condensation occurs [31]. In order to calculate the concentrations of POC and SOC in OC measured in the study area, the method of OC/EC minimum ratio [32] was employed as the following:

$$SOC = OC - (OC/EC)_{min} \times EC \quad (1)$$

$$POC = OC - SOC \quad (2)$$

where $(OC/EC)_{min}$ is the OC/EC minimum ratio found in $PM_{2.5}$ samples measured in the study area and EC and OC are the concentrations of elemental carbon and organic carbon determined in the $PM_{2.5}$ samples, respectively.

As the fractions of primary carbon might be strongly influenced by the source regions, source types, and atmospheric processes during different measurement periods, the OC/EC minimum ratios could be largely variable. For example, the OC/EC ratios of 0.8, 2.2, 4.15, 12.7, and 14.5 were reported for heavy-duty diesel vehicles, light-duty gasoline vehicles, wood combustion, natural gas home appliances, and forest fires, respectively [33]. In the present study, the OC/EC minimum ratio of 5.315 (seen on 10 July 2020) was used. A significantly positive correlation (R = 0.856) between OC and EC in the summer period implied the dominance of primary emission sources (i.e., traffic emissions, coal combustion). Therefore, the above OC/EC minimum ratio was applicable to estimate the concentrations of POC and SOC in the measured OC. The results for the daily concentrations of POC and SOC in the study areas are displayed in Figure 4. The concentrations of POC and SOC estimated for the summer period were 7.13 ± 4.11 μg m^{-3} and 4.72 ± 3.60 μg m^{-3}, respectively, which were about 60.16% and 39.84% of the OC concentration. Meanwhile, the counterparts for the winter period were 12.74 ± 4.79 μg m^{-3} and 17.46 ± 10.75 μg m^{-3}, respectively, accounting for 42.19% and 57.81% of the measured OC. These findings implied the larger contribution of secondary sources than that of primary sources to OC measured during the winter period, compared to those during the summer period.

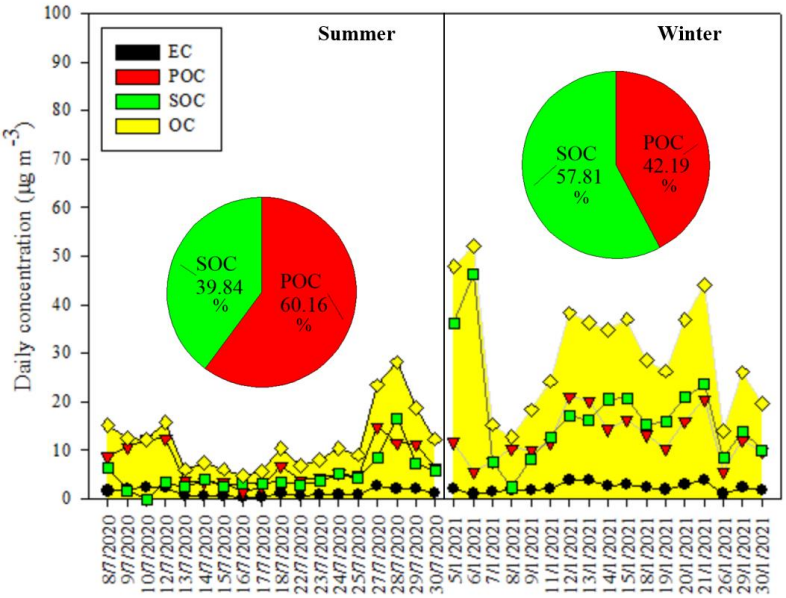

Figure 4. Daily variation of EC, OC, POC, and SOC concentration for the summer and winter periods.

In this study, organic mass (OM), a key component of $PM_{2.5}$, was calculated from the OC measured at the sampling site by multiplying the concentration of OC with a factor to account for the presence of oxygen and hydrogen atoms. According to [34], a factor of 1.6 ± 0.2 was recommended for urban areas worldwide [35,36]. Since there is currently no data reported for urban areas in Vietnam, the value of 1.6 was selected for the present study. The OM concentrations estimated for the summer and winter periods were 18.97 ± 10.28 μg m^{-3} and 51.34 ± 20.42 μg m^{-3} which accounted for 47.70% and 42.92% of the $PM_{2.5}$ total mass, respectively (Figure 3). This suggested that OM is one of the predominant species in ambient air in Hanoi City. However, it should be noted that adopting the factor of 1.6 to estimate the fraction of OM in the measured $PM_{2.5}$ could present some uncertainties. It is recommended that those uncertainties should be addressed in the future studies.

3.2. Analysis of Relationship among $PM_{2.5}$ Chemical Components

Analysis of the relationships between mass concentration of $PM_{2.5}$ and its chemical compositions would help to identify the key chemical species controlling the temporal variability of $PM_{2.5}$. The Pearson correlation coefficients among $PM_{2.5}$ species measured in the study area for the summer and winter periods were shown in Table 3. The results in Table 3 and the proportion of $PM_{2.5}$ chemical compositions (Figure 3) indicated that the daily variability of $PM_{2.5}$ was largely driven by OC (or OM) and EC (R = 0.725 and 0.689, respectively), and to a lesser extent by NO_3^- NH_4^+, and SO_4^{2-} (R = 0.598, 0.476, and 0.454, respectively), in the summer period. Meanwhile, OC (R = 0.835), followed by SO_4^{2-}, NH_4^+, K^+, Cl^-, and EC (R = 0.950, 0.914, 0.864, 0.649, and 0.387, respectively) were the main species controlling the daily variability of $PM_{2.5}$ in the winter period.

Table 3. Pearson correlation coefficients among $PM_{2.5}$ chemical compositions measured during the summer and winter periods.

	$PM_{2.5}$	F^-	Cl^-	NO_3^-	SO_4^{2-}	Na^+	NH_4^+	K^+	Mg^{2+}	Ca^{2+}	OC	EC
Summer												
$PM_{2.5}$	1.000	−0.167	0.572	0.598	0.454	−0.316	0.476	0.329	0.436	0.001	0.725	0.689
F^-		1.000	0.187	0.142	−0.014	0.327	0.072	0.292	−0.208	0.077	−0.072	−0.086
Cl^-			1.000	0.960	0.677	0.151	0.816	0.550	0.298	0.012	0.631	0.519
NO_3^-				1.000	0.742	0.180	0.840	0.349	0.534	0.056	0.660	0.450
SO_4^{2-}					1.000	−0.111	0.973	0.286	0.585	−0.409	0.829	0.536
Na^+						1.000	−0.043	−0.118	−0.054	0.509	−0.406	−0.526
NH_4^+							1.000	0.419	0.493	−0.345	0.824	0.574
K^+								1.000	−0.395	−0.369	0.465	0.717
Mg^{2+}									1.000	0.052	0.523	0.145
Ca^{2+}										1.000	−0.477	−0.538
OC											1.000	0.856
EC												1.000
Winter												
$PM_{2.5}$	1.000	0.793	0.649	0.074	0.950	0.637	0.914	0.864	0.787	0.641	0.835	0.387
F^-		1.000	0.601	−0.013	0.756	0.595	0.774	0.706	0.686	0.477	0.743	0.176
Cl^-			1.000	0.604	0.730	0.891	0.758	0.649	0.862	0.867	0.576	0.777
NO_3^-				1.000	0.179	0.433	0.185	0.253	0.515	0.539	0.228	0.624
SO_4^{2-}					1.000	0.704	0.983	0.888	0.836	0.770	0.758	0.491
Na^+						1.000	0.756	0.580	0.817	0.708	0.417	0.538
NH_4^+							1.000	0.860	0.814	0.780	0.711	0.477
K^+								1.000	0.818	0.730	0.835	0.404
Mg^{2+}									1.000	0.837	0.682	0.545
Ca^{2+}										1.000	0.541	0.769
OC											1.000	0.449
EC												1.000

Analysis of the correlation between cations and anions in $PM_{2.5}$ could suggest the atmospheric formation processes as well as the key sources for aerosol components [3]. According to [37], SO_4^{2-}, NO_3^-, and NH_4^+ are usually considered as the secondary species which are formed by the transformation of SO_2, NOx, and NH_3, respectively, in the atmosphere. As seen in Table 3, NH_4^+ was strongly correlated with SO_4^{2-} (R = 0.973 and R = 0.983 for the summer and winter periods, respectively). This suggested that there were common sources and/or processes influencing these two species in both the summer and

winter periods [38]. A relatively strong correlation between SO_4^{2-} and NO_3^- (R = 0.742) for the summer period implied that there was a common trend in source and atmospheric processes of two species. However, for the winter period, there was a low correlation between SO_4^{2-} and NO_3^- which suggested different sources and processes affecting the variation of these species. The mass ratio of NO_3^-/SO_4^{2-} has been widely applied to investigate the role of mobile sources (motor vehicle emissions) vs. stationary sources (emissions from coal combustion) in contributing to atmospheric $PM_{2.5}$ [39,40]. The high mass ratio of NO_3^-/SO_4^{2-} would suggest the predominant role of mobile sources over stationary sources, and vice versa [41]. Figure 5 indicated that the NO_3^-/SO_4^{2-} mass ratios measured for the summer period (mean ± standard deviation of 0.25 ± 0.21, range 0.02–0.69) were much higher than those for the winter period (mean ± standard deviation of 0.003 ± 0.002, range 0.001–0.008). These results implied the more important role of local traffic emission sources than that of stationary emission sources in contributing to anthropogenic air pollutants during the summer period in this study. However, emissions from stationary sources (i.e., coal burning for cement, steel, and coal-fired power plants in the surrounding provinces of Hanoi) were likely the significant sources of local air pollution through atmospheric transport process during the winter period (discussed in the later section). However, compared to the other studies, the NO_3^-/SO_4^{2-} mass ratios in this study were still lower than those reported for Beijing (0.71) [37], Shanghai (0.43) [40], and Qingdao (0.35) [42] in China.

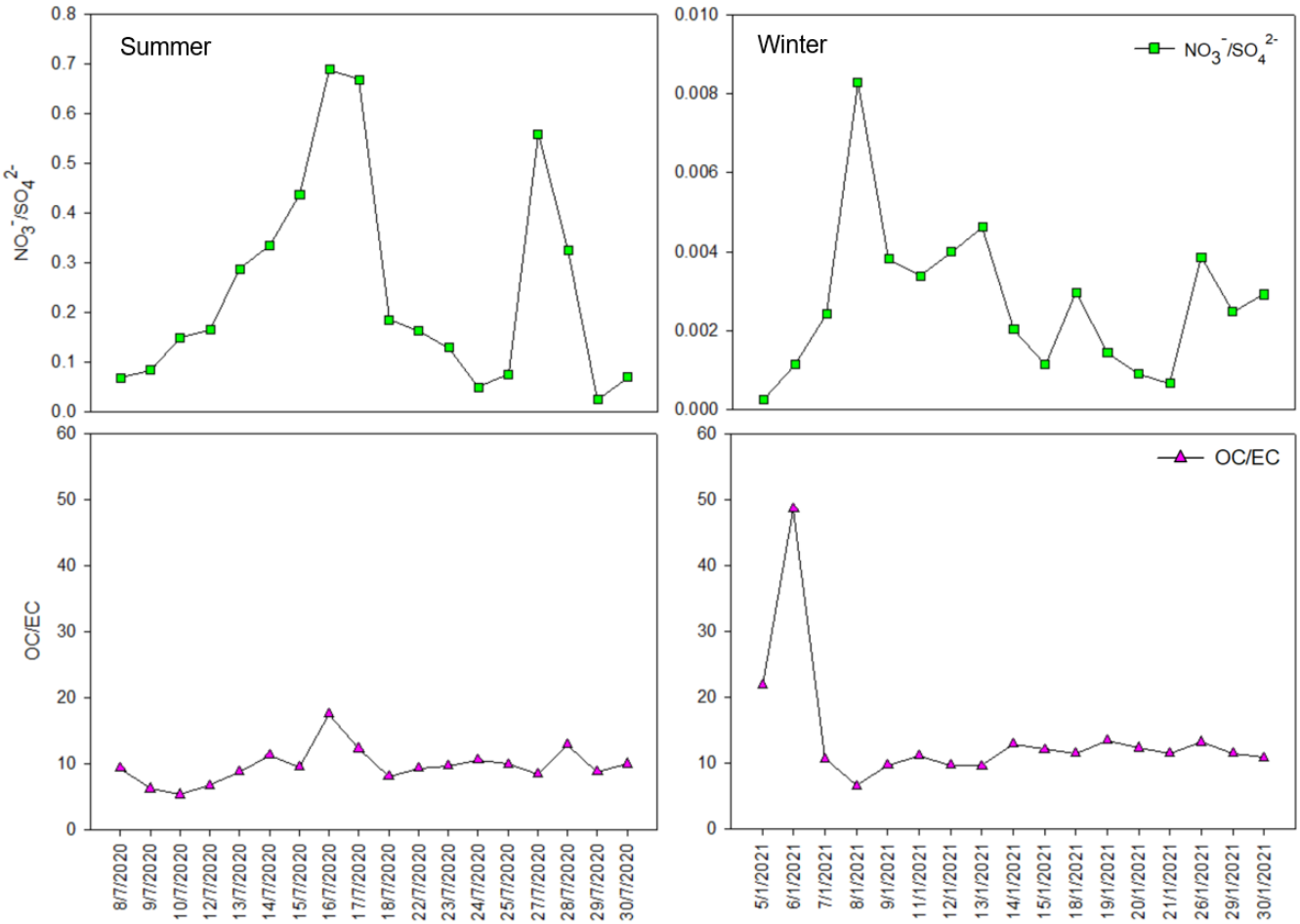

Figure 5. Daily variation of NO_3^-/SO_4^{2-} and OC/EC mass ratio for the summer and winter periods.

According to [43], atmospheric Mg^{2+} and Ca^{2+} usually originate from crustal sources (i.e., soil, construction, and re-suspended road dust). For the summer period, a slightly positive correlation between Mg^{2+} and Ca^{2+} was seen, which suggested that the sources

contributing to Mg^{2+} and Ca^{2+} during this period might be different. However, for the winter period, a significant positive correlation for Mg^{2+} and Ca^{2+} was found, which suggested the common crustal sources for these cations. For sea salt aerosol, a low correlation for Na^+ and NO_3^-/Cl^- were observed for the summer period. This was likely due to the fact that NO_3^-/Cl^- were firstly balanced with NH_4^+ as discussed above. Thus, after balancing with NH_4^+, the free NO_3^-/Cl^- were not significantly associated with Na^+. However, for the winter period, Na^+ was strongly correlated with Cl^-, while Na^+ was moderately correlated with NO_3^-. These results suggested the more important role of sea salt aerosol as a contributor to $PM_{2.5}$ measured for the winter period.

Because K^+, Cl^-, EC, and OC are commonly reported as the tracers for biomass burning activities [44,45], the possible influence of biomass burning sources on the $PM_{2.5}$ measured in the study area was assessed. As presented in Table 3, moderate positive correlations (K^+ vs. EC, K^+ vs. Cl^-, EC vs. Cl^-, OC vs. Cl^-) were found for both the summer and winter periods, which implied the possible impact of biomass burning source to the measured $PM_{2.5}$, which will be further explored in a later section. This point was also confirmed by the strong correlation between EC and OC (R = 0.856) for the summer period which implies that the key sources of EC and OC were somewhat similar for this period [46]. However, as SOC contributed more to the measured OC during the winter period (Figure 4), the strength of the correlation between OC and EC decreased for this period. It was reported that the emission sources for EC are mainly the primary sources and they are relatively stable. Whereas OC include both POC released directly from combustion and other sources and SOC formed by gas-to-particle transformation [47]. The OC/EC ratio has been widely used to assess the sources of carbonaceous species. For example, [48] reported the OC/EC ratios of 1.1, 2.7, and 9.0 for traffic emission, coal combustion, and biomass burning activities, respectively. In another study [49], the OC/EC ratios >2 were reported as the indicators for the formation of SOC. In the present study, the daily values of OC/EC ratio for the summer (mean ± standard deviation of 9.70 ± 2.75, range 5.32–17.58) and winter (mean ± standard deviation of 13.93 ± 9.46, range 6.55–48.64) periods were very high. This suggested that the high concentration of OC measured in the study area could be impacted by either SOC formation or biomass burning activities, as discussed in the above section. Furthermore, the highly variable OC/EC daily ratios (Figure 5) during both the summer and winter periods also suggested the possible impacts of complex sources and processes, changes in source regions or sources strengths, and different synoptic meteorological conditions during the study periods.

3.3. Influences of Seasonal Meteorological Conditions and Regional Fire Activities on the Variation of $PM_{2.5}$ and Its Chemical Compositions

In the present study, the relationships between meteorological parameters and mass concentrations of $PM_{2.5}$ as well as its major species (Table 4) were analyzed to gain a better understanding of the impact of seasonal meteorological conditions on atmospheric $PM_{2.5}$ measured in the study area. There were moderately positive correlations between relative humidity and $PM_{2.5}$ for both the summer and winter periods, which suggested that relative humidity played a certain role in enhancing $PM_{2.5}$ pollution in the study area. With respect to the major species in $PM_{2.5}$, SO_4^{2-} and NH_4^+ were positively correlated with relative humidity in both the summer and winter periods. A good positive correlation between SOC and relative humidity was also seen for the summer period. Since SO_4^{2-} and NH_4^+ are usually species with strong hygroscopicity [50,51], the relatively high relative humidity during both the summer and winter periods in the study area (Table 1) might enhance the hygroscopic growth of atmospheric particles and increase the aqueous-phase reactions [52,53]. It was reported that at the relative humidity >70%, the hygroscopic growth of atmospheric particles could strongly happen and the liquid water content in $PM_{2.5}$ was found to positively correlate with relative humidity, SO_4^{2-}, and NH_4^+ [10].

Table 4. Pearson correlation coefficients among $PM_{2.5}$, $PM_{2.5}$ chemical compositions, and meteorological parameters.

	Relative Humidity		Wind Speed		Boundary Layer Height		Ambient Temperature	
	Summer	**Winter**	**Summer**	**Winter**	**Summer**	**Winter**	**Summer**	**Winter**
$PM_{2.5}$	0.383	0.548	−0.701	−0.775	−0.749	−0.799	−0.483	0.462
Cl^-	0.488	0.401	−0.513	−0.748	−0.584	−0.769	−0.602	0.371
NO_3^-	0.551	−0.040	−0.518	−0.352	−0.574	−0.339	−0.652	0.092
SO_4^{2-}	0.751	0.577	−0.633	−0.793	−0.665	−0.794	−0.743	0.484
Na^+	−0.107	0.659	0.368	−0.753	0.493	−0.819	0.206	0.601
NH_4^+	0.720	0.644	−0.616	−0.817	−0.675	−0.839	−0.745	0.565
K^+	−0.042	0.438	−0.285	−0.743	−0.410	−0.766	−0.073	0.440
Mg^{2+}	0.456	0.512	−0.331	−0.750	−0.343	−0.776	−0.467	0.473
Ca^{2+}	−0.085	0.379	0.025	−0.582	0.158	−0.647	0.111	0.282
OC	0.512	0.128	−0.656	−0.704	−0.805	−0.688	−0.603	0.294
POC	0.171	−0.087	−0.478	−0.449	−0.685	−0.411	−0.348	−0.065
SOC	0.719	0.182	−0.626	−0.586	−0.655	−0.585	−0.680	0.358
EC	0.171	−0.087	−0.478	−0.449	−0.685	−0.411	−0.348	−0.065

When considering the impacts of wind speed on the variation of atmospheric $PM_{2.5}$ and its chemical components, the moderate to strong negative correlations between wind speed and $PM_{2.5}$ as well as most of $PM_{2.5}$ chemical species were generally observed for both the summer and winter periods. A similar result was also seen when examining the effects of boundary layer height on the variation of atmospheric $PM_{2.5}$. These findings implied that the higher values of wind speed and boundary layer height might lead to the enhanced atmospheric dispersion and in turn lead to reduced concentrations of air pollutants near the surface, and vice versa. In terms of seasonal variation, the lower values of wind speed and boundary layer height during the winter period (Table 1) were favorable for the trapping of air pollutants in the ground, and could contribute to the increased concentration of $PM_{2.5}$ and its chemical compositions in the winter period [54,55].

Table 4 showed the significant negative correlations between ambient temperature and the secondary species (NO_3^-, SO_4^{2-}, NH_4^+, and SOC) during the summer period. Since nitrate has a relatively high volatility, the high temperature in summer could increase its concentration in the gaseous phase, and thus cause the lower concentration in the particle phase. Ambient temperature generally also had moderate to strong negative correlations with concentration of the other species in $PM_{2.5}$. These results implied that the high temperature in the summer period could enhance the atmospheric convection, subsequently leading to the dilution and dispersion of air pollutants [56,57]. In contrast, during the winter period, there were the moderate positive correlations between ambient temperature and the secondary species (SO_4^{2-}, NH_4^+, and SOC). The previous studies [58,59] also showed the increased concentration of those secondary particles with the increased ambient temperature. The correlations between ambient temperature and $PM_{2.5}$ were similar to those for the secondary species (SO_4^{2-}, NH_4^+, and SOC) in the summer and winter periods since these species were the major contributors to $PM_{2.5}$ in both seasons in the study area.

In order to identify the possible impact of the distant sources located in the provinces near Hanoi, the relationship between wind direction and concentration of key chemical compositions in $PM_{2.5}$ was explored. During the summer period, the southeast wind was the most prevailing wind sector, followed by the south and east winds (Figure 6a). The highest concentrations of Cl^-, NO_3^-, Na^+, K^+, Ca^{2+}, and EC were corresponding to the southeast wind. Meanwhile, SO_4^{2-} and NH_4^+ reached their highest concentrations with respect to both the southeast and east winds, which suggested the common sources for these species during the summer period. The elevated concentrations of OC corresponded to the east wind. There are many large industrial sources (cement, steel, and coal-fired power plants) situated in the northern, eastern, and southern provinces near Hanoi (Figure 1). Thus, under certain meteorological conditions in the summer period, wind could bring air pollutants released from those sources towards the study area in Hanoi and contribute to the elevated concentrations of $PM_{2.5}$ and its chemical components. Meanwhile, the

dominant winds in the winter period were the southeast, northeast, and north winds (Figure 6b). The high concentrations of Cl^-, NH_4^+, and Ca^{2+} were related to the north wind. Meanwhile, the highest concentration of NO_3^- were associated with the southeast wind which was quite similar to that in the summer period. The highest concentrations of SO_4^{2-} and Na^+ were found with both the southeast and north winds. K^+ showed its diverse source regions in the winter period, where its highest concentrations were seen more frequently with the southeast wind, followed by the north, northeast, and east winds. The highest concentrations of OC and EC were seen with the northeast and southeast winds, respectively. From these results, it could be inferred that in addition to the southeast wind, either the north or northeast winds might partly contribute to the increased concentration of $PM_{2.5}$ in the winter period via the transport of air pollutants released from the regional sources to the study area. In summary, the change in seasonal wind directions, and subsequently the change in the source regions, could influence the variation of concentration of $PM_{2.5}$ and its major species in the study area.

Biomass burning has been reported as one of the important regional and/or local sources of poor air quality in Southeast Asian countries [10,31,60–68]. As an effort to further identify the source regions of fires associated with the seasonal air masses which influence the seasonal variation of atmospheric $PM_{2.5}$, the integrated maps of MODIS cumulative FRP and air mass trajectories at the measurement site for the summer period (July 2020) and winter period (January 2021) are displayed in Figure 7. It was observed that during the summer period, air masses originated from the south, southwest, and southeast directions, and passed over both the continental (central region of Vietnam, Laos, and Thailand) and maritime (the East Sea) environment before arriving at the sampling site in Hanoi. On the other hand, air masses mainly originating from the north and northeast directions travelled through the Pearl River Delta region in the southern part of China (a highly industrialized area) before arriving at the measurement site during the winter period. The MODIS fire maps showed that fire sources occurring in the southern part of China and the Southeast Asia region (Vietnam, Laos, Thailand, and Myanmar) during the winter period were much more intensive than those during the summer period. As air masses traveled across the highly industrialized and intensive fire regions during the winter period, they might have carried a large amount of air pollutants, released from those regional sources, to the study area and resulted in the highly elevated concentrations of $PM_{2.5}$ and its anthropogenic/biomass burning species (SO_4^{2-}, NH_4^+, K^+, OC, and EC, as presented in Table 1). The strong impact of long-range transport on the local $PM_{2.5}$ pollution has been also reported by the other studies [10,64,65,69]. In contrast, the occurrence of air masses passing through the maritime environment (which was not strongly influenced by anthropogenic sources) and the less intensive fire regions during the summer period was identified as the main reason for the lower concentrations of $PM_{2.5}$ and its anthropogenic/biomass burning species (SO_4^{2-}, NH_4^+, K^+, EC, and OC) and the higher concentrations of species associated with seawater (Na^+ and Mg^{2+}).

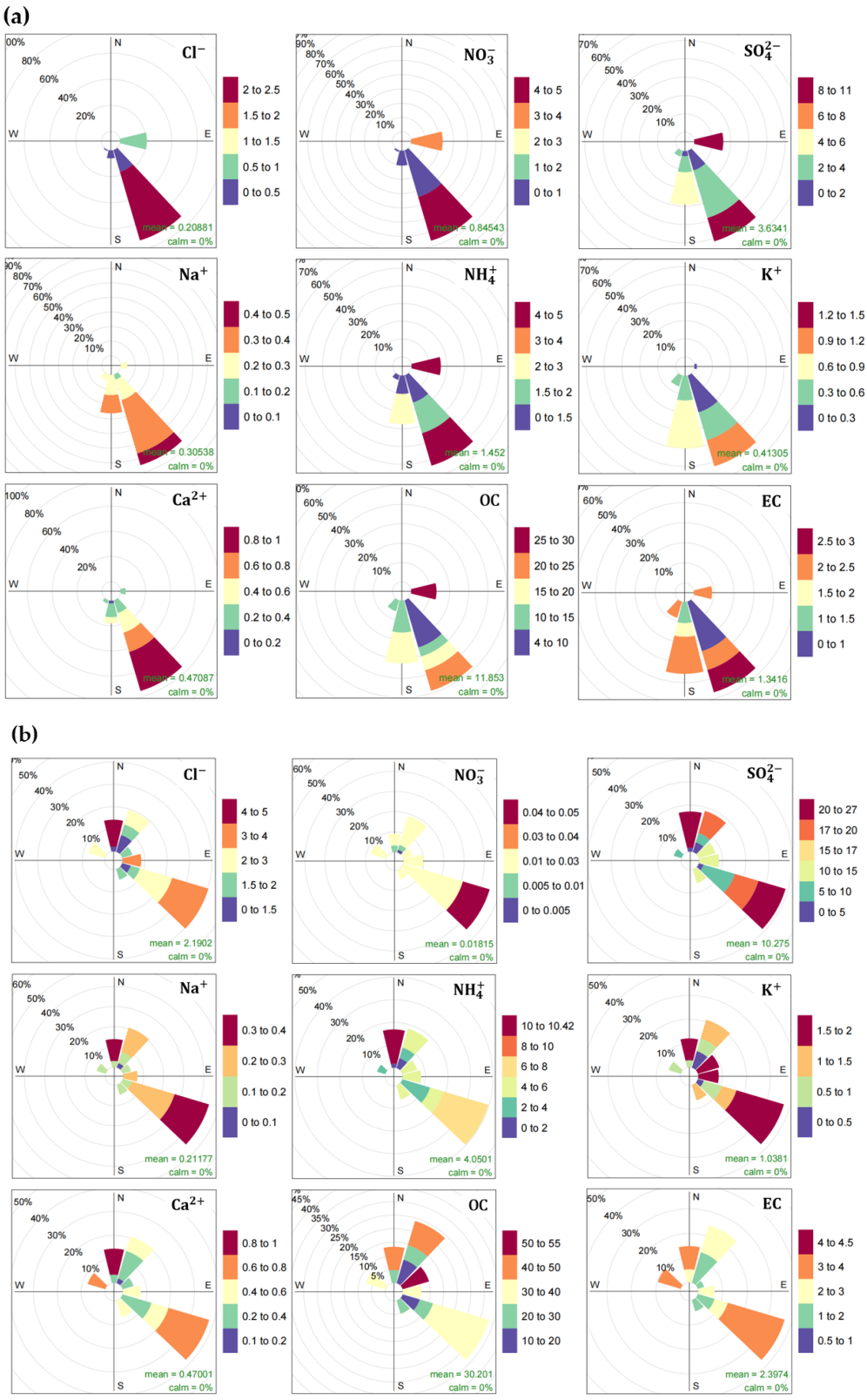

Figure 6. Spatial pattern of concentration of key chemical compositions in $PM_{2.5}$ in relation to wind direction during: (**a**) summer period; (**b**) winter period (for interpretation of the references to color in this figure legend, the reader is referred to the web version of this article).

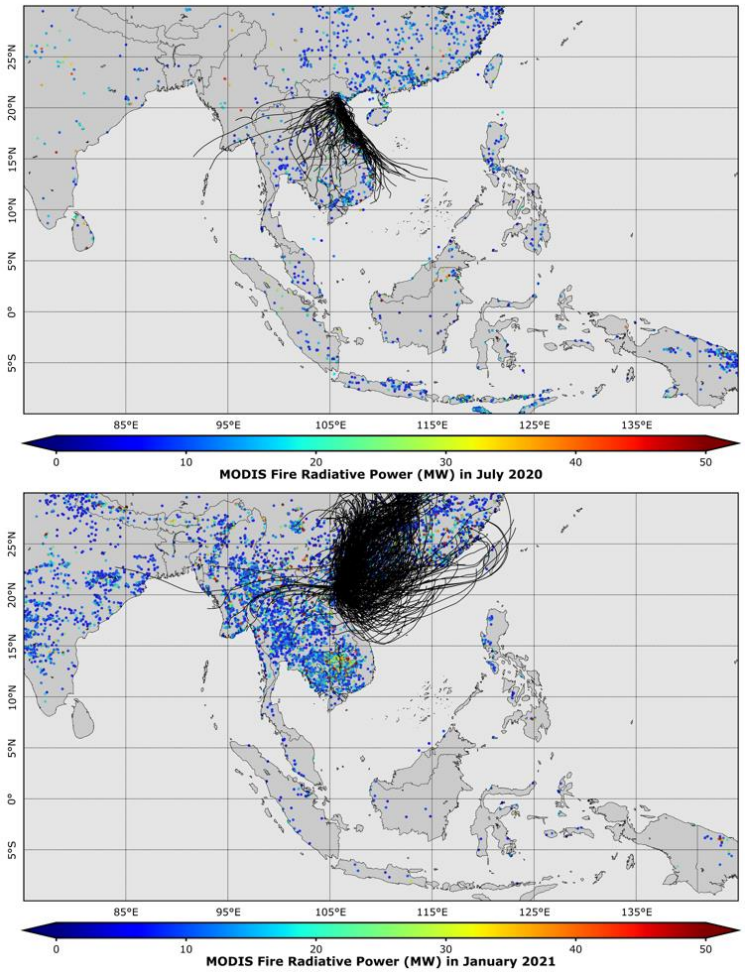

Figure 7. MODIS cumulative fire radiative power over the Southeast Asian region and three-day air mass backward trajectories (indicated by the black curves) arrived at the sampling site in Hanoi during the summer period (July 2020) and winter period (January 2021).

4. Conclusions

In this study, the seasonal variation and chemical characteristics of atmospheric $PM_{2.5}$ in an urban area of Hanoi City, Vietnam were investigated. The two intensive $PM_{2.5}$ sampling campaigns were carried out for summer (July 2020) and winter (January 2021) periods. Based on the findings of this study, the following key conclusions can be drawn:

- The concentration of $PM_{2.5}$ and its key components (Cl^-, SO_4^{2-}, NH_4^+, K^+, OC, and EC) measured in the winter period were significantly higher than those measured in the summer period, implying heavy $PM_{2.5}$ pollution in the winter period.
- The estimation of SOC showed the larger contribution of secondary sources than of primary sources to OC observed during the winter period, compared to those in the summer period.
- The correlation analysis among anions and cations in atmospheric $PM_{2.5}$ suggested that different sources and atmospheric processes could influence the seasonal variations of $PM_{2.5}$ species.
- The analysis of the relationship between meteorological parameters and mass concentrations of $PM_{2.5}$, as well as its major species, demonstrated that the unfavorable meteorological condition (lower wind speed and lower boundary-layer height) in the winter period was one of the key factors contributing to the increased $PM_{2.5}$ pollution in this season.

- Due to the dominance of north and northeast winds during the winter period, the impact of long-range transport of air pollutants emitting from the largely industrialized and intensive fire regions in the southern China and Southeast Asia region was likely another important source for the increased $PM_{2.5}$ pollution in the winter period.

Author Contributions: Conceptualization, writing—original draft, Q.T.B. and D.L.N.; data, visualization, Q.T.B.; data analysis, D.L.N. and T.H.B.; review and editing, T.H.B. All authors have read and agreed to the published version of the manuscript.

Funding: This research received funding from Vietnam Ministry of Education and Training (MOET) under the grant number B2020-XDA-04.

Institutional Review Board Statement: Not applicable.

Informed Consent Statement: Not applicable.

Data Availability Statement: The data presented in this study are available on reasonable request from the corresponding author.

Acknowledgments: The authors would like to thank MOET for providing the financial support for this research under the grant number B2020-XDA-04. The authors also would like to thank the Laboratory for Analysis and Control of Environmental Pollution, Faculty of Environment, University of Science, Vietnam National University Ho Chi Minh City, Vietnam for the support in carbonaceous analysis. The authors gratefully acknowledge the NOAA Air Resources Laboratory for the provision of the HYSPLIT trajectory model and/or READY website (https://www.ready.noaa.gov/HYSPLIT.php, accessed on 12 May 2021) used in this publication.

Conflicts of Interest: The authors declare no conflict of interest.

References

1. Katsouyanni, K.; Touloumi, G.; Samoli, G.; Gryparis, A.; Le Tertre, A.; Monopolis, Y.; Rossi, G.; Zmirou, D.; Ballester, F.; Boumghar, A.; et al. Confounding and effect modification in the short-term effects of ambient particles on total mortality: Results from 29 European cities within the APHEA2 project. *Epidemiology* **2011**, *12*, 521–531. [CrossRef] [PubMed]
2. Pope, C.A.; Dockery, D.W. Health effects of fine particulate air pollution: Lines that connect. *J. Air Waste Manag. Assoc.* **2006**, *56*, 709–742. [CrossRef] [PubMed]
3. Eleftheriadis, K.; Klaus, M.O.; Theopisti, L.; Angeliki, K.; Panayiotis, R.; Maria, O.P. Influence of local and regional sources on the observed spatial and temporal variability of size resolved atmospheric aerosol mass concentrations and water-soluble species in the Athens metropolitan area. *Atmos. Environ.* **2014**, *97*, 252–261. [CrossRef]
4. Danalatos, D.; Glavas, S. Gas phase nitric acid, ammonia and related particulate matter at a Mediterranean coastal site, Patras, Greece. *Atmos. Environ.* **1999**, *33*, 3417–3425. [CrossRef]
5. Querol, X.; Alastuey, A.; Rodriguez, S.; Plana, F.; Ruiz, C.R.; Cots, N.; Massague, G.; Puig, O. PM_{10} and $PM_{2.5}$ source apportionment in the Barcelona metropolitan area Catalonia Spain. *Atmos. Environ.* **2010**, *35*, 6407–6419. [CrossRef]
6. Zhu, L.; Daven, K.H.; Jesse, O.B.; Karen, E.C.P.; Mark, W.S.; Ming, L.; Shannon, L.C. Sources and Impacts of Atmospheric NH3: Current Understanding and Frontiers for Modeling Measurements and Remote Sensing in North America. *Curr. Pollut. Rep.* **2015**, *1*, 95–116. [CrossRef]
7. Chen, J.; Chunlin, L.; Zoran, R.; Andelija, M.; Yuantong, G.; Mohammad, S.I.; Shuxiao, W.; Jiming, H.; Hefeng, Z.; Congrong, H.; et al. A review of biomass burning: Emissions and impacts on air quality, health and climate in China. *Sci. Total Environ.* **2017**, *579*, 1000–1034. [CrossRef]
8. Reiss, R.; Anderson, E.L.; Cross, C.E.; Hidy, G.; Hoel, D.; McClellan, R.; Moolgavkar, S. Evidence of health impacts of sulfate-and-nitrate-containing particles in ambient air. *Inhal. Toxicol.* **2007**, *19*, 419–449. [CrossRef]
9. World Bank. Available online: https://www.worldbank.org/en/country/vietnam/overview (accessed on 18 April 2022).
10. Nguyen, D.L.; Hieu, B.T.; Trung, B.Q.; Dat, M.V.; Duy, N.V.; Dinh, P.V.; Hien, T.T.; Hiep, N.H. Investigation of sources and processes influencing variation of $PM_{2.5}$ and its chemical compositions during a summer period of 2020 in an urban area of Hanoi city, Vietnam. *Air. Qual. Atmos. Health.* **2022**, *15*, 235–253. [CrossRef]
11. Ministry of Natural Resources and Environment (MONRE). *Report on the Implementation of National Action Plan on Air Quality Management to 2020, Vision to 2025*; 2020. (In Vietnamese)
12. CEM. *Air Quality Report for Hanoi City in 2019*; Vietnam Environment Administration, Ministry of Natural Resources and Environment: Hanoi, Vietnam, 2019. (In Vietnamese)
13. Nguyen, D.L.; Nowarat, C. Strategic environmental assessment application for sustainable transport-related air quality policies: A case study in Hanoi City Vietnam. *Environ. Dev. Sustain.* **2011**, *13*, 565–585. [CrossRef]

14. Tran, N.Q.; Nguyen, T.H.; Mac, V.D.; Tran, L.K.; Thai, H.P.; Morawska, L.; Thai, K.P. Motorcyclists have much higher exposure to black carbon compared to other commuters in traffic of Hanoi, Vietnam. *Atmos. Environ.* **2021**, *245*, 118–129. [CrossRef]
15. Sakamoto, Y.; Shoji, K.; Bui, M.T.; Pham, T.H.; Vu, T.A.; Ly, B.T.; Kajii, Y. Air quality study in Hanoi, Vietnam in 2015–2016 based on a one-year observation of NOx, O3, CO and a one-week observation of VOCs. *Atmos. Pollut. Res.* **2018**, *9*, 544–551. [CrossRef]
16. Giglio, L.; Schroeder, W.; Justice, C.O. The collection 6 MODIS active fire detection algorithm and fire products. *Remote Sens. Environ.* **2016**, *178*, 31–41. [CrossRef] [PubMed]
17. Draxler, R.R.; Rolph, G.D. *HYSPLIT (HYbrid SINGLE-Particle Lagrangian Integrated Trajectory)*; Model Access, NOAA Air Resources Laboratory, Silver Spring; 2019. Available online: http://www.arl.noaa.gov/ready/hysplit4.html (accessed on 18 March 2022).
18. Ahmed, M.; Guo, X.X.; Xing, M.Z. Determination and analysis of trace metals and surfactant in air particulate matter during biomass burning haze episode in Malaysia. *Atmos. Environ.* **2016**, *141*, 219–229. [CrossRef]
19. Sulong, N.A.; Latif, M.T.; Khan, M.F.; Amil, N.; Ashfold, M.J.; Wahab, M.I.A.; Sahani, M. Source apportionment and health risk assessment among specific age groups during haze and non-haze episodes in Kuala Lumpur Malaysia. *Sci. Total Environ.* **2017**, *601*, 556–570. [CrossRef]
20. Dahari, N.; Latif, M.T.; Muda, K.; Hussein, N. Influence of Meteorological Variables on Suburban Atmospheric $PM_{2.5}$ in the Southern Region of Peninsular Malaysia. *Aerosol Air. Qual. Res.* **2020**, *20*, 14–25. [CrossRef]
21. Alias, N.F.; Khan, M.F.; Sairi, N.A.; Zain, S.M.; Suradi, H.; Rahim, H.A.; Tirthankar, B.; Aynul Bari, M.; Murnira, O.; Mohd, T.L. Characteristics, emission sources, and risk factors of heavy metals in $PM_{2.5}$ from southern Malaysia. *ACS Earth Space Chem.* **2020**, *4*, 1309–1323. [CrossRef]
22. Zhang, Z.; Khlystov, A.; Norford, L.K.; Tan, Z.; Balasubramanian, R. Characterization of traffic-related ambient fine particulate matter ($PM_{2.5}$) in an Asian city: Environmental and health implications. *Atmos. Environ.* **2017**, *161*, 132–143. [CrossRef]
23. ChooChuay, C.; Siwatt, P.; Danai, T.; Oramas, S.; Woranuch, D.; Qiyuan, W.; Li, X.; Guohui, L.; Yongming, H.; Jittree, P.; et al. Impacts of $PM_{2.5}$ sources on variations in particulate chemical compounds in ambient air of Bangkok, Thailand. *Atmos. Pollut. Res.* **2020**, *11*, 1657–1667. [CrossRef]
24. Santoso, M.; Lestiani, D.D.; Kurniawati, S.; Damastuti, E.; Kusmartini, I.; Atmodjo, D.P.D.; Sari, D.K.; Hopke, P.K.; Mukhtar, R.; Muhtarom, T.; et al. Assessment of Urban Air Quality in Indonesia. *Aerosol Air. Qual. Res.* **2020**, *20*, 2142–2158. [CrossRef]
25. Hien, T.T.; Chi, N.D.T.; Nguyen, N.T.; Vinh, L.X.; Takenaka, N.; Huy, D.H. Current Status of Fine Particulate Matter ($PM_{2.5}$) in Vietnam's Most Populous City, Ho Chi Minh City. *Aerosol Air. Qual. Res.* **2019**, *19*, 2239–2251. [CrossRef]
26. Zeng, J.; Zhang, L.; Yao, C.; Xie, T.; Rao, L.; Lu, H.; Liu, X.; Wang, Q.; Lu, S. Relationships between chemical elements of PM2.5 and O3 in Shanghai atmosphere based on the 1-year monitoring observation. *J. Environ. Sci.* **2020**, *95*, 49–57. [CrossRef] [PubMed]
27. Luo, L.; Bai, X.; Liu, S.; Wu, B.; Liu, W.; Lv, Y.; Guo, Z.; Lin, S.; Zhao, S.; Hao, Y.; et al. Fine particulate matter ($PM_{2.5}/PM_{1.0}$) in Beijing, China: Variations and chemical compositions as well as sources. *J. Environ. Sci.* **2022**, *121*, 187–198. [CrossRef] [PubMed]
28. Thepnuan, D.; Chantara, S. Characterization of PM2.5–bound Polycyclic Aromatic Hydrocarbons in Chiang Mai Thailand during Biomass Open Burning Period of 2016. *Appl. Environ. Res.* **2020**, *42*, 11–24. [CrossRef]
29. Ravindra, K.; Singh, T.; Sinha, V.; Sinha, B.; Paul, S.; Attri, S.D.; Mor, S. Appraisal of regional haze event and its relationship with $PM_{2.5}$ concentration, crop residue burning and meteorology in Chandigarh, India. *Chemosphere* **2021**, *273*, 128562. [CrossRef]
30. Jain, S.; Sharma, S.K.; Srivastava, M.K.; Chatterjee, A.; Vijayan, N.; Tripathy, S.S.; Kumari, K.M.; Mandal, T.K.; Sharma, C. Chemical characterization, source apportionment and transport pathways of PM2.5 and PM10 over Indo Gangetic Plain of India. *Urban Clim.* **2021**, *36*, 100805. [CrossRef]
31. Nguyen, D.L.; Viet, H.T.; Hieu, B.T.; Trung, B.Q.; Ha, V.V. Evaluating carbonaceous species in fine particle $PM_{2.5}$ in an urban area in Hanoi. *J. Sci. Technol. Civ. Eng. STCE-HUCE* **2021**, *15*, 9–17. [CrossRef]
32. Siciliano, T.; Siciliano, M.; Malitesta, C.; Proto, A.; Cucciniello, R.; Giove, A.; Iacobellis, S.; Genga, A. Carbonaceous PM_{10} and $PM_{2.5}$ and secondary organic aerosol in a coastal rural site near Brindisi (Southern Italy). *Environ. Sci. Pollut. Res.* **2018**, *25*, 23929–23945. [CrossRef]
33. Volkamer, R.; Jimenez, J.L.; Martini, F.S.; Dzepina, K.; Zhang, Q.; Salcedo, D.; Molina, L.T.; Worsnop, D.R.; Molina, M.J. Secondary organic aerosol formation from anthropogenic air pollution: Rapid and higher than expected. *Geophys. Res. Lett.* **2006**, *33*, L17811. [CrossRef]
34. Turpin, B.J.; Lim, H.J. Species contributions to $PM_{2.5}$ mass concentrations: Revisiting common assumptions for estimating organic mass. *Aerosol Sci. Technol.* **2001**, *35*, 602–610. [CrossRef]
35. Huang, X.F.; Yun, H.; Gong, Z.H.; Li, X.; He, L.Y.; Zhang, Y.H.; Hu, M. Source apportionment and secondary organic aerosol estimation of $PM_{2.5}$ in an urban atmosphere in China. *Sci. China Earth Sci.* **2014**, *57*, 1352–1362. [CrossRef]
36. Mancilla, Y.; Herckes, P.; Fraser, M.P.; Mendoza, A. Secondary organic aerosol contributions to PM2.5 in Monterrey Mexico: Temporal and seasonal variation. *Atmos. Res.* **2015**, *153*, 348–359. [CrossRef]
37. Wang, Y.; Zhuang, G.S.; Tang, A.H.; Yuan, H.; Sun, Y.L.; Chen, S.; Zheng, A. The ion chemistry and the source of $PM_{2.5}$ aerosol in Beijing. *Atmos. Environ.* **2005**, *39*, 3771–3784. [CrossRef]
38. Mirante, F.; Salvador, P.; Pio, C.; Alves, C.; Artiñano, B.; Caseiro, A.; Revuelt, M.A. Size fractionated aerosol composition at roadside and background environments in the Madrid urban atmosphere. *Atmos. Res.* **2014**, *138*, 278–292. [CrossRef]
39. Arimoto, R.; Duce, R.A.; Savoie, D.L.; Prospero, J.M.; Talbot, R.; Cullen, J.D.; Tomza, U.; Lewis, N.F.; Ray, B.J. Relationships among aerosol constituents from Asia and the North Pacific during Pem-West A. *J. Geophys. Res. Atmos.* **1996**, *101*, 2011–2023. [CrossRef]

40. Yao, X.; Chan, C.K.; Fang, M.; Cadle, S.; Chan, T.; Mulawa, P.; He, K.; Ye, B. The water-soluble ionic composition of $PM_{2.5}$ in Shanghai and Beijing, China. *Atmos. Environ.* **2002**, *36*, 4223–4234. [CrossRef]
41. Cao, J.J.; Zhenxing, S.; Judith, C.C.; Guowei, Q.; John, G.W. Seasonal variations and sources of mass and chemical composition for PM_{10} aerosol in Hangzhou, China. *Particuology* **2009**, *7*, 161–168. [CrossRef]
42. Hu, M.; He, L.; Zhang, Y.; Wang, M.; Kim, Y.P.; Moon, K.C. Seasonal variation of ionic species in fine particles at Qingdao, China. *Atmos. Environ.* **2002**, *36*, 5853–5859. [CrossRef]
43. Sun, Z.; Yujing, M.; Yanju, L.; Longyi, S. A comparison study on airborne particles during haze days and non-haze days in Beijing. *Sci. Total Environ.* **2013**, *456–457*, 1–8. [CrossRef]
44. Adachi, K.; Buseck, P.R. Internally mixed soot, sulfates, and organic matter in aerosol particles from Mexico City. *Atmos. Chem. Phys.* **2008**, *8*, 6469–6481. [CrossRef]
45. Reid, J.S.; Koppmann, R.; Eck, T.F.; Eleuterio, D.P. A review of biomass burning emissions part II: Intensive physical properties of biomass burning particles. *Atmos. Chem. Phys.* **2005**, *5*, 799–825. [CrossRef]
46. Cao, J.J.; Lee, S.C.; Chow, J.C.; Ho, K.F.; Zhang, X.Y.; Zou, S.C.; Fung, K.K.; Chow, J.C.; Watson, J.G. Characteristics of carbonaceous aerosol in Pearl River Delta Region, China during 2001 winter period. *Atmos. Environ.* **2003**, *37*, 1451–1460. [CrossRef]
47. Wang, P.; Cao, J.J.; Shen, Z.X.; Han, Y.M.; Lee, S.C.; Huang, Y.; Zhu, C.S.; Wang, Q.Y.; Xu, H.M.; Huang, R.J. Spatial and seasonal variations of PM2.5 mass and species during 2010 in Xi'an China. *Sci. Total Environ.* **2015**, *508*, 477–487. [CrossRef] [PubMed]
48. Watson, J.G.; Chow, J.C.; Houck, J.E. $PM_{2.5}$ chemical source profiles for vehicle exhaust vegetative burning geological material and coal burning in Northwestern Colorado during 1995. *Chemosphere* **2001**, *43*, 1141–1151. [CrossRef]
49. Hildemann, L.M.; Markowski, G.R.; Cass, G.R. Chemical composition of emissions from urban sources of organic aerosol. *Environ. Sci. Technol.* **1991**, *25*, 744–759. [CrossRef]
50. Bai, Z.; Ji, Y.; Pi, Y.; Yang, K.; Wang, L.; Zhang, Y.; Zhai, Y.; Yan, Z.G.; Han, X.D. Hygroscopic analysis of individual Beijing haze aerosol particles by environmental scanning electron microscopy. *Atmos. Environ.* **2018**, *172*, 149–153. [CrossRef]
51. Sjogren, S.; Gysel, M.; Weingartner, E.; Baltensperger, U.; Cubison, M.J.; Coe, H.; Zardini, A.A.; Marcolli, C.; Krieger, U.K.; Peter, T. Hygroscopic growth and water uptake kinetics of two-phase aerosol particles consisting of ammonium sulfate adipic and humic acid mixtures. *J. Aerosol Sci.* **2007**, *38*, 157–171. [CrossRef]
52. Liu, F.; Tan, Q.; Jiang, X.; Yang, F.; Jiang, W. Effects of relative humidity and PM2.5 chemical compositions on visibility impairment in Chengdu China. *J. Environ. Sci.* **2019**, *86*, 15–23. [CrossRef]
53. Ma, Q.; Wu, Y.; Zhang, D.; Wang, X.; Xia, Y.; Liu, X.; Tian, P.; Han, Z.; Xia, X.; Wang, Y.; et al. Roles of regional transport and heterogeneous reactions in the PM2.5 increase during winter haze episodes in Beijing. *Sci. Total Environ.* **2017**, *599–600*, 246–253. [CrossRef]
54. Lim, H.J.; Turpin, B.J. Origins of primary and secondary organic aerosol in Atlanta: Results of time-resolved measurements during the Atlanta supersite experiment. *Environ. Sci. Technol.* **2002**, *36*, 4489–4496. [CrossRef]
55. Qiao, T.; Zhao, M.; Xiu, G.; Yu, J. Simultaneous monitoring and compositions analysis of PM_1 and $PM_{2.5}$ in Shanghai: Implications for characterization of haze pollution and source apportionment. *Sci. Total Environ.* **2016**, *557–558*, 386–394. [CrossRef] [PubMed]
56. Luo, J.; Du, P.; Samat, A.; Xia, J.; Che, M.; Xue, Z. Spatiotemporal Pattern of $PM2_{.5}$ Concentrations in Mainland China and Analysis of Its Influencing Factors using Geographically Weighted Regression. *Sci. Rep.* **2017**, *7*, 40607. [CrossRef] [PubMed]
57. Yang, Q.; Yuan, Q.; Li, T.; Shen, H.; Zhang, L. The Relationships between $PM_{2.5}$ and Meteorological Factors in China: Seasonal and Regional Variations. *Int. J. Environ. Res. Public Health.* **2017**, *14*, 1510. [CrossRef] [PubMed]
58. Pateraki, S.; Asimakopoulos, D.N.; Flocas, H.A.; Maggos, T.; Vasilakos, C. The role of meteorology on different sized aerosol fractions (PM10, PM2.5, PM2.5–10). *Sci. Total Environ.* **2012**, *419*, 124–135. [CrossRef] [PubMed]
59. Vassilakos, C.; Pateraki, S.; Veros, D.; Maggos, T.; Michopoulos, J.; Saraga, D.; Helmis, C.G. Temporal determination of heavy metals in PM2.5 aerosols in a suburban site of Athens, Greece. *J. Atmos. Chem.* **2007**, *57*, 1–17. [CrossRef]
60. Bui, T.H.; Nguyen, D.L.; Nguyen, H.H.; Bui, Q.T. Comparison of aerosol products retrieved from AERONET and MODIS over an urban area in Hanoi city, Vietnam. *J. Sci. Technol. Civ. Eng. STCE-HUCE* **2018**, *12*, 99–108. [CrossRef]
61. Bui, T.H.; Nguyen, D.L.; Nguyen, H.H. Study of aerosol optical properties at two urban areas in the north of Vietnam with the implication for biomass burning impacts. *Environ. Sci. Pollut. Res.* **2021**, *29*, 41923–41940. [CrossRef]
62. Bui, T.H.; Nguyen, D.L.; Nguyen, H.H.; Bui, Q.T.; Do, H.D. Inter-comparison between MODIS satellite-based and AERONET ground-based Aerosol Optical Depth products in Viet Nam. *Vietnam. J. Sci. Technol.* **2020**, *58*, 124–132. [CrossRef]
63. Huang, K.; Fu, J.S.; Hsu, N.C.; Gao, Y.; Dong, X.; Tsay, S.C.; Lam, Y.F. Impact assessment of biomass burning on air quality in Southeast and East Asia during BASE-ASIA. *Atmos. Environ.* **2012**, *78*, 291–302. [CrossRef]
64. Lasko, K.; Vadrevu, K.P.; Tran, V.T.; Ellicott, E.; Nguyen, T.T.N.; Bui, H.Q.; Justice, C. Satellites may underestimate rice residue and associated burning emissions in Vietnam. *Environ. Res. Lett.* **2017**, *12*, 085006. [CrossRef]
65. Nguyen, D.L.; Hieu, B.T.; Hiep, N.H. Contrasting seasonal pattern between ground-based $PM_{2.5}$ and MODIS satellite-based aerosol optical depth (AOD) at an urban site in Hanoi, Vietnam. *Environ. Sci. Pollut. Res.* **2022**, *29*, 41971–41982. [CrossRef]
66. Nguyen, D.L.; Hieu, B.T.; Vy, V.H.; Thuy, P.T. Studying the optical and physical properties of aerosol in an urban area of Hanoi City. *Version B Vietnam. J. Sci. Technol.* **2022**, *64*, 1–6. [CrossRef]
67. Trung, B.Q.; Nguyen, D.L.; Hieu, B.T.; Dat, M.V.; Duy, N.V.; Chinh, P.M.; Viet, H.T. Evaluating concentration of element and carbon in atmospheric PM10 measured in an urban area in Hanoi during summer 2020. *J. Sci. Technol. Civ. Eng. STCE-HUCE* **2021**, *15*, 62–70. [CrossRef]

68. Trung, B.Q.; Nguyen, D.L.; Hieu, B.T.; Dat, M.V.; Duy, N.V.; Chinh, P.M.; Viet, H.T.; Hoa, H.X. Evaluating ionic and carbonaceous species in fine particle PM2.5 measured during winter in an urban area in Hanoi. *J. Sci. Technol. Civ. Eng. STCE-HUCE* **2022**, *16*, 54–64. [CrossRef]
69. Ngoc, B.A.P.; Delbarre, H.; Deboudt, K.; Dieudonné, E.; Tran, D.N.; Thanh, S.L.; Pelon, J.; Ravetta, F. Key factors explaining severe air pollution espisodes in Hanoi during 2019 winter season. *Atmos. Pollut. Res.* **2021**, *12*, 101068. [CrossRef]